DOI: 10.1021/ic900673s

Inorganic Chemistry
Article

Luminescent Boron-Contained Ladder-Type π-Conjugated Compounds

Zuolun Zhang,[†] Hai Bi,[†] Yu Zhang,[†] Dandan Yao,[†] Hongze Gao,[†] Yan Fan,[†] Hongyu Zhang,*[,†] Yue Wang,*[,†] Yanping Wang,[‡] Zhenyu Chen,[‡] and Dongge Ma[‡]

[†]*State Key Laboratory of Supramolecular Structure and Materials, College of Chemistry, Jilin University, Changchun 130012, P.R. China, and* [‡]*State Key Laboratory of Polymer Physics and Chemistry, Changchun Institute of Applied Chemistry, Graduate School of the Chinese Academy of Sciences, Chinese Academy of Sciences, Changchun 130022, P.R. China*

Received April 6, 2009

Four diboron-contained ladder-type π-conjugated compounds **1**−**4** were designed and synthesized. Their thermal, photophysical, electrochemical properties, as well as density functional theory calculations, were fully investigated. The single crystals of compounds **1** and **3** were grown, and their crystal structures were determined by X-ray diffraction analysis. Both compounds have a ladder-type π-conjugated framework. Compounds **1** and **2** possess high thermal stabilities, moderate solid-state fluorescence quantum yields, as well as stable redox properties, indicating that they are possible candidates for emitters and charge-transporting materials in electroluminescent (EL) devices. The double-layer device with the configuration of [ITO/NPB (40 nm)/**1** or **2** (70 nm)/LiF (0.5 nm)/Al (200 nm)] exhibited good EL performance with the maximum brightness exceeding 8000 cd/m^2.

Introduction

Ladder-type π-conjugated compounds are a class of materials with flat and rigid skeletons that lead to a set of desirable properties such as a strong luminescence and a high carrier mobility, which are important for high-performance organic electronic and optoelectronic devices including organic light-emitting diodes (OLEDs), transistors, and lasers.[1] Recently, the ladder π-conjugated systems bearing main group elements such as silicon, sulfur, selenium, phosphorus, boron, and nitrogen have attracted much attention and proved to be an efficient way to modulate their electronic and optical properties.[2−6]

Four-coordinate boron compounds reported by other groups and us have proved to be promising emitters in electroluminescent (EL) devices.[7−9] In addition, some of these compounds exhibit certain electron-transporting

*To whom correspondence should be addressed. E-mail: hongyuzhang@jlu.edu.cn (H.Z.), yuewang@jlu.edu.cn (Y.W.).

(1) (a) Watson, M. D.; Fechtenkötter, A.; Müllen, K. *Chem. Rev.* **2001**, *101*, 1267. (b) Anthony, J. E. *Chem. Rev.* **2006**, *106*, 5028. (c) Scherf, U. *J. Mater. Chem.* **1999**, *9*, 1853.

(2) (a) Yamaguchi, S.; Xu, C.; Tamao, K. *J. Am. Chem. Soc.* **2003**, *125*, 13662. (b) Xu, C.; Wakamiya, A.; Yamaguchi, S. *J. Am. Chem. Soc.* **2005**, *127*, 1638. (c) Xu, C.; Wakamiya, A.; Yamaguchi, S. *Org. Lett.* **2004**, *6*, 3707. (d) Mouri, K.; Wakamiya, A.; Yamada, H.; Kajiwara, T.; Yamaguchi, S. *Org. Lett.* **2007**, *9*, 93.

(3) (a) Okamoto, T.; Kudoh, K.; Wakamiya, A.; Yamaguchi, S. *Chem.—Eur. J.* **2007**, *13*, 548. (b) Takimiya, K.; Kunugi, Y.; Konda, Y.; Ebata, H.; Toyoshima, Y.; Otsubo, T. *J. Am. Chem. Soc.* **2006**, *128*, 3044. (c) Wong, K.-T.; Chao, T.-C.; Chi, L.-C.; Chu, Y.-Y.; Balaiah, A.; Chiu, S.-F.; Liu, Y.-H.; Wang, Y. *Org. Lett.* **2006**, *8*, 5033. (d) Takimiya, K.; Ebata, H.; Sakamoto, K.; Izawa, T.; Otsubo, T.; Kunugi, Y. *J. Am. Chem. Soc.* **2006**, *128*, 12604. (e) Yamamoto, T.; Takimiya, K. *J. Am. Chem. Soc.* **2007**, *129*, 2224.

(4) (a) Fukazawa, A.; Hara, M.; Okamoto, T.; Son, E.-C.; Xu, C.; Tamao, K.; Yamaguchi, S. *Org. Lett.* **2008**, *10*, 913. (b) Fukazawa, A.; Yamada, H.; Yamaguchi, S. *Angew. Chem., Int. Ed.* **2008**, *47*, 5582.

(5) (a) Agou, T.; Kobayashi, J.; Kawashima, T. *Chem. Commun.* **2007**, 3204. (b) Agou, T.; Kobayashi, J.; Kawashima, T. *Org. Lett.* **2006**, *8*, 2241. (c) Agou, T.; Kobayashi, J.; Kawashima, T. *Chem.—Eur. J.* **2007**, *13*, 8051. (d) Agou, T.; Kobayashi, J.; Kawashima, T. *Org. Lett.* **2005**, *7*, 4373.

(6) (a) Kawaguchi, K.; Nakano, K.; Nozaki, K. *J. Org. Chem.* **2007**, *72*, 5119. (b) Bouchard, J.; Wakim, S.; Leclerc, M. *J. Org. Chem.* **2004**, *69*, 5705. (c) Patil, S. A.; Scherf, U.; Kadashchuk, A. *Adv. Funct. Mater.* **2003**, *13*, 609. (d) Wakim, S.; Bouchard, J.; Blouin, N.; Michaud, A.; Leclerc, M. *Org. Lett.* **2004**, *6*, 3413. (e) Kaszynski, P.; Dougherty, D. A. *J. Org. Chem.* **1993**, *58*, 5209.

(7) (a) Wu, Q.; Esteghamatian, M.; Hu, N.-X.; Popovic, Z.; Enright, G.; Tao, Y.; Diorio, M.; Wang, S. *Chem. Mater.* **2000**, *12*, 79. (b) Liu, Q.; Mudadu, M. S.; Schmider, H.; Thummel, R.; Tao, Y.; Wang, S. *Organometallics.* **2002**, *21*, 4743. (c) Cui, Y.; Liu, Q.-D.; Bai, D.-R.; Jia, W.-L.; Tao, Y.; Wang, S. *Inorg. Chem.* **2005**, *44*, 601. (d) Liu, Q.-D.; Mudadu, M. S.; Thummel, R.; Tao, Y.; Wang, S. *Adv. Funct. Mater.* **2005**, *15*, 143. (e) Wang, S. *Coord. Chem. Rev.* **2001**, *215*, 79. (f) Liu, S.-F.; Wu, Q.; Schmider, H. L.; Aziz, H.; Hu, N.-X.; Popovic, Z.; Wang, S. *J. Am. Chem. Soc.* **2000**, *122*, 3671.

(8) (a) Hellstrom, S. L.; Ugolotti, J.; Britovsek, G. J. P.; Jones, T. S.; White, A. J. P. *New J. Chem.* **2008**, *32*, 1379. (b) Chen, H.-Y.; Chi, Y.; Liu, C.-S.; Yu, J.-K.; Cheng, Y.-M.; Chen, K.-S.; Chou, P.-T.; Peng, S.-M.; Lee, G.-H.; Carty, A. J.; Yeh, S.-J.; Chen, C.-T. *Adv. Funct. Mater.* **2005**, *15*, 567. (c) Chen, T.-R.; Chien, R.-H.; Jan, M.-S.; Yeh, A.; Chen, J.-D. *J. Organomet. Chem.* **2006**, *691*, 799. (d) Kappaun, S.; Rentenberger, S.; Pogantsch, A.; Zojer, E.; Mereiter, K.; Trimmel, G.; Saf, R.; Möller, K. C.; Stelzer, F.; Slugovc, C. *Chem. Mater.* **2006**, *18*, 3539. (e) Chen, T.-R.; Chien, R.-H.; Yeh, A.; Chen, J.-D. *J. Organomet. Chem.* **2006**, *691*, 1998.

(9) (a) Li, Y.; Liu, Y.; Bu, W.; Guo, J.; Wang, Y. *Chem. Comm.* **2000**, 1551. (b) Feng, J.; Li, F.; Gao, W. B.; Liu, S. Y.; Liu, Y.; Wang, Y. *Appl. Phys. Lett.* **2001**, *78*, 3947. (c) Liu, Y.; Guo, J.; Zhang, H.; Wang, Y. *Angew. Chem., Int. Ed.* **2002**, *41*, 182. (d) Zhang, H.; Huo, C.; Ye, K.; Zhang, P.; Tian, W.; Wang, Y. *Inorg. Chem.* **2006**, *45*, 2788. (e) Zhang, H.; Huo, C.; Zhang, J.; Zhang, P.; Tian, W.; Wang, Y. *Chem. Commun.* **2006**, 281.

Published on Web 06/25/2009

properties, so that they were employed to fabricate simple double-layer EL devices; however, the performance of these devices was usually not satisfactory. To achieve high EL performance, the devices based on this type of materials usually need additional electron-transporting materials, which usually make the fabrication processes tedious and thus increase the cost of the production of OLEDs.[8a−8c,9d] Therefore, it is a very important issue to develop boron materials appropriate for fabricating structurally simple and high-performance EL devices. Recently, Yamaguchi and coworkers reported that the diboron-contained ladder π-system can increase not only the electron affinity but also the fluorescence efficiency compared with the monoboron species.[10] This result indicates that incorporating multiboron centers in a rigid conjugated π-system is an ideal synthetic strategy to endow this system with strong electron-accepting character and high fluorescence quantum yield. However, only few rigid mutiboron-contained π-systems, such as ladder-type boron-contained systems, have been achieved to date probably because of the lack of efficient synthetic routes.

In this study, we design and synthesize four ladder-type compounds containing two boron atoms in the π-conjugated skeleton. We suspect that compounds with such a molecular structure would be the light-emitting materials with transporting properties. The X-ray single crystal structures, thermal stabilities, photophysical and electrochemical properties of these compounds have been investigated. To demonstrate their application potentials in OLEDs, the EL properties of some of these compounds are also presented.

Experimental Section

General Information. All starting materials were purchased from Aldrich Chemical Co. and used without further purification. The solvents for syntheses were freshly distilled over appropriate drying reagents. All experiments were performed under a nitrogen atmosphere by using standard Schlenk techniques. ^{1}H NMR spectra were measured on Bruker AVANCE 500 MHz spectrometer with tetramethylsilane as the internal standard. Mass spectra were recorded on a Shimadzu AXIMA-CFR MALDI-TOF mass spectrometer. Elemental analyses were performed on a flash EA 1112 spectrometer. Differential scanning calorimetric (DSC) measurements were performed on a NETZSCH DSC204 instrument. Thermogravimetric analyses (TGA) were performed on a TA Q500 thermogravimeter. UV−vis absorption spectra were recorded using a PE UV−vis lambdazo spectrometer. The emission spectra were recorded using a Shimadzu RF-5301 PC spectrometer. Tri-(8-hydroxyquinolino)aluminum (Alq_3) was purchased from Aldrich and purified by vacuum sublimation. *N*,*N*′-di(1-naphthyl)-*N*,*N*′-diphenyl-(1,1′-biphenyl)-4,4′-diamine (NPB),[11] 2,5-bis(2-pyridyl)-1,4-hydroquinone (H_2L1), 2,5-bis(5-methyl-2-pyridyl)-1,4-hydroquinone (H_2L2),[12] and 2-(2-pyridyl) phenol (HL3)[13] were synthesized according to the literature procedures.

$Ph_2B(\mu$-L1)BPh_2 (1). A solution of BPh_3 (303 mg, 1.25 mmol) in THF (10 mL) was added to a solution of H_2L1 (150 mg, 0.57 mmol) in THF (20 mL) at room temperature, and then the reaction mixture was stirred overnight at the same temperature. The reaction mixture was concentrated to about 5 mL by vacuum, and 50 mL of petroleum ether was added. The resulting suspension was filtered, and the solid was purified by vacuum sublimation to give compound **1** as orange solid (215 mg, 64% yield). ^{1}H NMR (DMSO, ppm): δ 8.51 (d, J = 8.0 Hz, 2 H), 8.34 (t, J = 7.5 Hz, 2 H), 8.14 (d, J = 5.5 Hz, 2 H), 7.73−7.71 (m, 4 H), 7.16−7.13 (m, 20 H). Ms m/z: 593.0 $[M]^+$ (calcd: 592.2). Anal. Calcd (%) for $C_{40}H_{30}B_2N_2O_2$: C, 81.11; H, 5.11; N, 4.73. Found: C, 81.13; H, 4.81; N, 4.69.

$Ph_2B(\mu$-L2)BPh_2 (2). In the same manner as described for **1**, the reaction of H_2L2 (80 mg, 0.28 mmol) and BPh_3 (144 mg, 0.60 mmol) provided **2** as an orange solid (92 mg, 54% yield). ^{1}H NMR (DMSO, ppm): δ 8.41 (d, J = 8.5 Hz, 2 H), 8.18 (d, J = 8.0 Hz, 2 H), 7.91 (s, 2 H), 7.67 (s, 2 H), 7.16−7.10 (m, 20 H), 2.35 (s, 6 H). Ms m/z: 620.3 $[M]^+$ (calcd: 620.3). Anal. Calcd (%) for $C_{42}H_{34}B_2N_2O_2$: C, 81.32; H, 5.52; N, 4.52. Found: C, 81.14; H, 5.77; N, 4.33.

$(C_2H_5)_2B(\mu$-L1)$B(C_2H_5)_2$ (3). In the same manner as described for **1**, the reaction of H_2L1 (200 mg, 0.76 mmol) and B$(C_2H_5)_3$ (1.67 mL, 1 M in THF, 1.67 mmol) provided **3** as an orange solid (173 mg, 57% yield). ^{1}H NMR ($CDCl_3$, ppm): δ 8.31 (d, J = 6.0 Hz, 2 H), 8.00−7.95 (m, 4 H), 7.44 (t, J = 6.5 Hz, 2 H), 7.35 (s, 2 H), 0.75 (t, J = 7.5 Hz, 12 H), 0.64−0.53 (m, 8 H). Ms m/z: 400.1 $[M]^+$ (calcd: 400.3). Anal. Calcd (%) for $C_{24}H_{30}B_2N_2O_2$: C, 72.04; H, 7.56; N, 7.00. Found: C, 71.93; H, 7.76; N, 6.86.

$(C_2H_5)_2B(\mu$-L2)$B(C_2H_5)_2$ (4). In the same manner as described for **1**, the reaction of H_2L2 (100 mg, 0.34 mmol) and B$(C_2H_5)_3$ (0.75 mL, 1 M in THF, 0.75 mmol) provided **4** as red-orange solid (77 mg, 53% yield). ^{1}H NMR ($CDCl_3$, ppm): δ 8.09 (s, 2 H), 7.85 (d, J = 8.5 Hz, 2 H), 7.78 (d, J = 8.0 Hz, 2 H), 7.30 (s, 2 H), 2.45 (s, 6 H), 0.75 (t, J = 7.5 Hz, 12 H), 0.61−0.53 (m, 8 H). Ms m/z: 428.3 $[M]^+$ (calcd: 428.3). Anal. Calcd (%) for $C_{26}H_{34}B_2N_2O_2$: C, 72.93; H, 8.00; N, 6.54. Found: C, 72.72; H, 7.73; N, 6.56.

Ph_2BL3 (5). A solution of BPh_3 (139 mg, 0.57 mmol) in THF (10 mL) was added to a solution of HL3 (82 mg, 0.48 mmol) in THF (20 mL) at room temperature, and then the reaction mixture was stirred overnight at the same temperature. The solvent was removed by vacuum, and the residue was purified by column chromatography (silica gel, CH_2Cl_2/cyclohexane 3:1) to give compound **5** as light green solid (129 mg, 80% yield). ^{1}H NMR (DMSO, ppm): δ 8.40 (d, J = 8.5 Hz, 1 H), 8.32 (t, J = 7.5 Hz, 1 H), 8.10 (d, J = 5.5 Hz, 1 H), 7.94 (d, J = 8.0 Hz, 1 H), 7.67 (t, J = 6.5 Hz, 1 H), 7.40 (t, J = 7.5 Hz, 1 H), 7.17−7.11 (m, 10 H), 7.06 (d, J = 8.0 Hz, 1 H), 6.88 (t, J = 7.5 Hz, 1 H). Ms m/z: 335.2 $[M]^+$ (calcd: 335.1). Anal. Calcd (%) for $C_{23}H_{18}BNO$: C, 82.41; H, 5.41; N, 4.18. Found: C, 82.40; H, 5.41; N, 4.07.

X-ray Diffraction. Diffraction data were collected on a Rigaku RAXIS-PRID diffractometer using the ω-scan mode with graphite-monochromator Mo·Kα radiation. The structures were solved with direct methods using the SHELXTL programs and refined with full-matrix least-squares on F^2. Non-hydrogen atoms were refined anisotropically. The positions of hydrogen atoms were calculated and refined isotropically.

Photoluminescent (PL) Quantum Yield Measurements. The fluorescence quantum yields in solution were measured relative to quinine sulfate in sulfuric acid aqueous solution (λ_{exc} = 365 nm, Φ_F = 0.546) at room temperature. For compounds **1**−**5**, the longest absorption maximum was chosen as the excitation wavelength. The quantum yields were calculated using previously known procedures.[14] The solid-state quantum yields were measured from the freshly evaporated film using an integrating sphere with the excitation wavelength of 409 nm for all the compounds.

Electrochemical Measurements. Cyclic voltammetry was performed on a BAS 100W instrument with a scan rate of 100 mV/s.

(10) Zhao, Q.; Zhang, H.; Wakamiya, A.; Yamaguchi, S. *Synthesis* **2009**, 127.
(11) Koene, B. E.; Loy, D. E.; Thompson, M. E. *Chem. Mater.* **1998**, *10*, 2235.
(12) Shu, W.; Valiyaveettil, S. *Chem. Commun.* **2002**, 1350.
(13) Li, Y.; Liu, Y.; Bu, W.; Lu, D.; Wu, Y.; Wang, Y. *Chem. Mater.* **2000**, *12*, 2672.
(14) Ye, K.; Wang, J.; Sun, H.; Liu, Y.; Mu, Z.; Li, F.; Jiang, S.; Zhang, J.; Zhang, H.; Wang, Y.; Che, C. M. *J. Phys. Chem. B.* **2005**, *109*, 8008.

A three-electrode configuration was used for the measurement: a platinum electrode as the working electrode, a platinum wire as the counter electrode, and an Ag/Ag^+ electrode as the reference electrode. A 0.1 M solution of tetrabutylammonium perchlorate (TBAP) in DMF or CH_2Cl_2 was used as the supporting electrolyte.

Theoretical Calculations. The ground state geometries were fully optimized by the density functional theory (DFT)[15] method with the Becke three-parameter hybrid exchange and the Lee−Yang−Parr correlation functional[16] (B3LYP) and 6-31G* basis set using the Gaussian 03 software package.[17]

Fabrication of EL Devices. Indium−tin oxide (ITO) coated glass was used as the substrate. It was cleaned by sonication successively in a detergent solution, acetone, methanol, and deionized water before use. The devices were prepared in vacuum at a pressure of 5×10^{-6} Torr. Organic layers were deposited onto the substrate at a rate of 1−2 Å/s. After the organic film deposition, LiF and aluminum were thermally evaporated onto the organic surface. The thicknesses of the organic materials and the cathode layers were controlled using a quartz crystal thickness monitor. The electrical characteristics of the devices were measured with a Keithley 2400 source meter. The EL spectra and luminance of the devices were obtained on a PR650 spectrometer.

Results and Discussion

Syntheses and Crystal Structures. The synthetic procedures for **1**−**4** are shown in Scheme 1. Simple mixing of the ligands (H_2L1 or H_2L2) and boron reagents in THF and subsequent purification by vacuum sublimation gave the targets **1**−**4** in moderate yields (53−64%). For comparison purposes, the monoboron compound **5** was also synthesized in 80% yield.

The single crystal structures of compounds **1** and **3** were determined by X-ray crystallography. The crystal lattices of **1** and **3** belong to triclinic $P\bar{1}$ space group, in which both molecules have a center of symmetry. Figure 1 shows the Oak Ridge thermal ellipsoid plot (ORTEP) drawing of **3**, and the ORTEP structure of **1** is shown in Supporting Information, Figure S6 [We failed in the attempt to obtain the better single crystals of compound **1** using several methods. The crystal was always too small to be used in the X-ray diffraction analysis. Although we finally got a small crystal suitable for the X-ray analysis, the diffractions were weak, which led to the high *R* indices.]. Boron atoms adopt a typical tetrahedral geometry, and the boron-contained six-membered rings take a chair conformation in which the boron atoms deviate from the central benzene plane by 0.69 Å for **1** and 0.72 Å for **3**. The B−N, B−O, and B−C bond lengths (Supporting Information, Table S2) of **1** and **3** are similar to those of the organoboron quinolates reported previously.[7a] The dihedral angles between the terminal pyridine plane and the central benzene plane are 14.53° in **1** and 16.83° in **3**, indicating that the ladder skeletons have certain distortions from the coplanar framework. There is no interfacial $\pi-\pi$ interaction in the packing structure of **1** probably because of the large steric hindrance of the peripheral phenyl rings, and this structural feature should play an important role to reduce the excimer formation in the solid state as already observed in ladder-type structures.[3c,18] In contrast, **3** forms a slipped face-to-face packing structure in which the interfacial $\pi-\pi$ distance of the adjacent molecules is about 3.5 Å (Supporting Information, Figure S7).

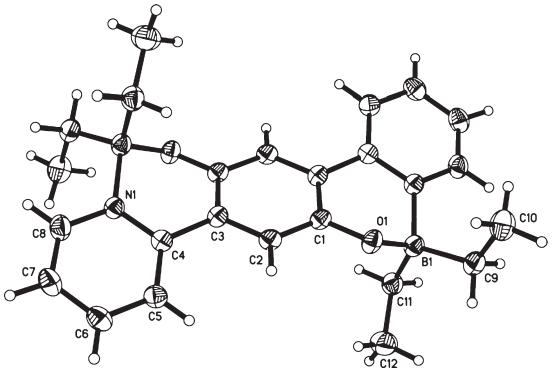

Figure 1. ORTEP drawing of **3** with 30% thermal ellipsoids.

Scheme 1. Synthetic Procedures for Compounds **1**−**5**

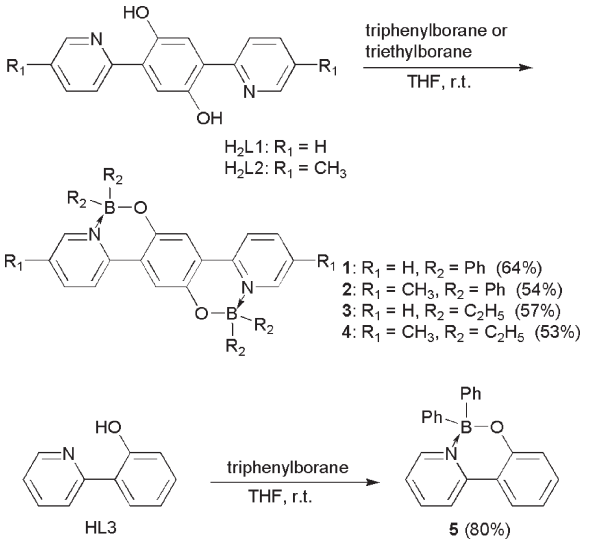

Thermal Analyses. We used thermogravimetric analysis (TGA) and differential scanning calorimetry (DSC) to characterize the thermal properties of **1**−**5** under a nitrogen atmosphere (Figure 2). The decomposition temperatures with a 5% weight loss (T_{d5}) for **1**−**5** are 378, 350, 268, 234, and 247 °C, respectively. Compounds **1** and **2** having aryl groups on the boron centers show much higher T_{d5} values compared with compounds **3** and **4** in which boron centers are substituted by flexible alkyl chains. This comparison clearly shows the significant effect of the substituents attached to the boron centers. We also note that the thermal stability of diboron compound **1** is greatly improved when compared with that of the monoboron compound **5**, indicative of the effect of the extended π-conjugation. It is believed that compounds **1**−**4** had already partially decomposed before melting in the DSC examinations considering that the

(15) Runge, E.; Gross, E. K. U. *Phys. Rev. Lett.* **1984**, *52*, 997.
(16) Becke, A. D. *J. Chem. Phys.* **1993**, *98*, 5648.
(17) Frisch, M. J. et al. *Gaussian 03*, Revision C.02; Gaussian, Inc.: Pittsburgh, PA, 2003.
(18) Wong, K.-T.; Chi, L.-C.; Huang, S.-C.; Liao, Y.-L.; Liu, Y.-H.; Wang, Y. *Org. Lett.* **2006**, *8*, 5029.

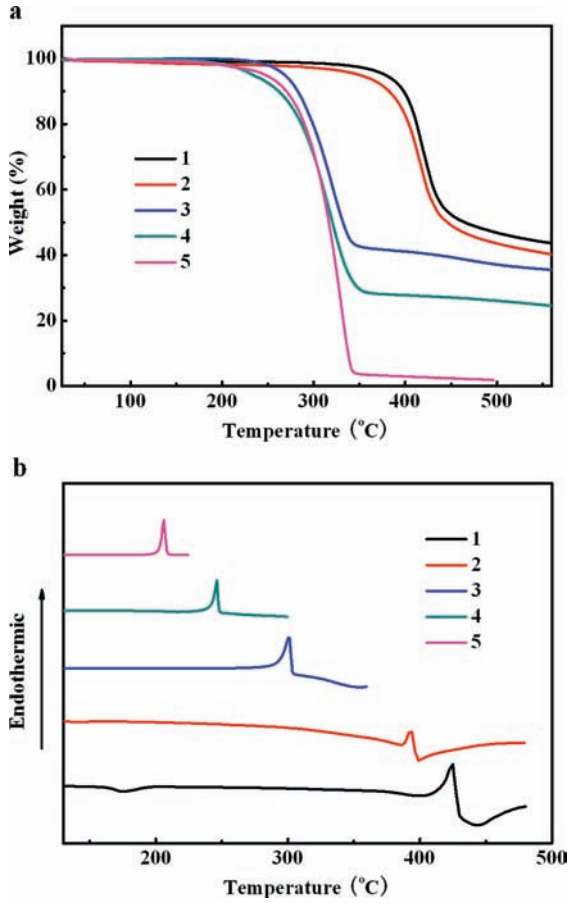

Figure 2. TGA (a) and DSC (b) curves of **1**−**5** at a heating rate of 10 °C/min.

measured melting points of these compounds (425, 393, 301, and 246 °C for **1**−**4**, respectively) are higher than their decomposition temperatures. The second cycles of the DSC measurement were not carried out because the melting of compounds **1**−**4** was accompanied by decomposition in the first cycles, and thus whether these compounds possess a glass transition temperature (T_g) could not be determined. The TGA and DSC data indicate that the ladder compounds **1** and **2** are highly thermally stable and would be capable of enduring the vacuum thermal sublimation process during OLED fabrication.

Optical Properties. The absorption and fluorescence spectra of **1**−**4** were recorded in THF. Their data are summarized in Table 1, together with the spectra data of **5**, H_2L1, and H_2L2 for comparison. In the UV−vis absorption spectra (Figure 3), all compounds **1**−**4** exhibit broad peaks around 450−480 nm, which are greatly red-shifted compared with those of the ligands. Such a red-shifted absorption caused by boron chelation was often observed in four-coordinate boron systems.[19] In comparison with **5** (λ_{max} = 361 nm), compound **1** with the absorption maximum of 461 nm exhibits an obvious red shift, which might be due to the increased effective conjugation length. The absorption maximum of ethyl-substituted derivative **3** is red-shifted by about 18 nm

(19) (a) Ren, Y.; Liu, X.; Gao, W.; Xia, H.; Ye, L.; Mu, Y. *Eur. J. Inorg. Chem.* **2007**, 1808. (b) Liddle, B. J.; Silva, R. M.; Morin, T. J.; Macedo, F. P.; Shukla, R.; Lindeman, S. V.; Gardinier, J. R. *J. Org. Chem.* **2007**, *72*, 5637.

Table 1. Photophysical Properties of Compounds **1**−**5**, H_2L1, and H_2L2

		λ_{em} (nm)		Φ_F	
compd	λ_{abs}, nm[a,b] (log ε)	solution[a]	film[c]	solution[a]	film[c]
1	461 (3.94)	584	584	0.29	0.18
2	455 (4.00)	578	579	0.30	0.22
3	479 (3.84)	611	562	0.08	0.13
4	473 (3.95)	604	587	0.08	0.14
5	361 (3.80)	481	448	0.34	0.39
H_2L1	398 (4.15)				
H_2L2	394 (4.17)				

[a] Data were collected in THF (3×10^{-6} M). [b] Only the longest absorption maxima are shown. [c] Thin film on quartz substrate with the thickness of about 100 nm.

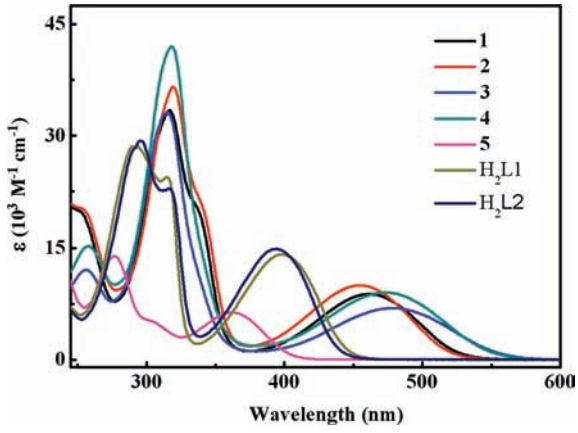

Figure 3. UV−vis absorption spectra of **1**−**5**, H_2L1, and H_2L2 in THF.

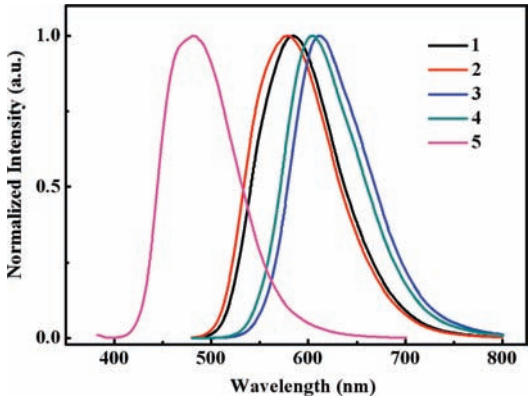

Figure 4. Emission spectra of **1**−**5** in THF.

compared with that of phenyl-substituted derivative **1**, and the same red shift is observed in the comparison between **4** and **2**, indicating that the electron-donating substituents on boron centers have great influence on the photophysical characteristics. Methyl groups on the ligand (compounds **2** and **4**) only have a subtle influence on the longest absorption maxima, leading to a blue shift of about 6 nm from the non-substituted to the methyl-substituted compounds.

Although the ligands H_2L1 and H_2L2 are non-emissive, compounds **1**−**4** show fluorescence in both solution and solid state. Figure 4 shows the fluorescence spectra of **1**−**5** in tetrahydrofuran (THF). The emission maxima of compounds **1**−**4** are located in the orange to red region,

being 584, 578, 611, and 604 nm, respectively. The emission maximum of **1** is obviously red-shifted by about 103 nm in comparison with that of **5**, which reflects the influence of the extended π-conjugation. In addition, the emission maxima of compounds **1**−**4** show a trend consistent with that of the observed energy gaps determined by UV−vis spectra. The fluorescence quantum yields of **1** and **2** determined by using quinine sulfate as reference are 0.29 and 0.30, respectively. These values are comparable to that of **5** (Φ_F = 0.34). In contrast, compounds **3** and **4** show very weak emission in solution (quantum yield for both **3** and **4** is 0.08). In the solid state, the emission peaks of compounds **1**−**4** are found at 584, 579, 562, and 587 nm, respectively. The emission spectra of **1** and **2** in the solid state are almost identical to those observed in solution. This data indicates that although the π-systems have ladder-type framework, the bulky phenyl groups attached to boron centers prevent efficient π-stacking in their aggregated state, which was also explained by the X-ray structure analysis. Moreover, in view of the application as emitting materials, compounds **1** and **2** might be promising because this feature makes it possible for these compounds to maintain the moderate solid-state fluorescence quantum yields in the solid state. Indeed, the quantum yields of the thin films reach 0.18 and 0.22 for **1** and **2**, respectively, which are relatively higher than those of the reported diboron-contained π-conjugated systems.[20] Compounds **3** and **4** display blue-shifted emissions in the solid state as compared with the solutions, which is probably due to the luminescence rigidchromism.[21]

Electrochemical Properties. The electrochemical properties of compounds **1**−**5** and the ligands H_2L1 and H_2L2 were studied by means of cyclic votammetry. Their cyclic voltammograms are shown in Figure 5 and the data are summarized in Table 2. These data are discussed from the viewpoints of (1) effect of conjugation length; (2) effect of boron chelation; and (3) effect of substituents attached to boron atom.

While the monoboron compound **5** displays an irreversible reduction wave with peak potential (E_{pc}) at −2.24 V, all diboron compounds **1**−**4** exhibit two sequential reversible reduction waves with the first half-wave potentials ($E_{red}^{1/2}$) at −1.81 ∼ −2.03 V (vs Fc/Fc^+). This result demonstrates that extension of the π-system from monoboron to diboron not only make the cathodic reductions easier but also stabilizes the produced radical anions. The consecutive peaks observed in the reductions of all ladder compounds are likely associated to the two boron chelating parts considering that there is only one reduction peak appearing in the cyclic voltammogram of the monoboron compound. For the free ligands H_2L1 and H_2L2, only one well resolved quasi-reversible reduction wave can be observed within the electrochemical window of *N*, *N*-dimethylformamide (DMF). The first reduction potentials of boron compounds **1**−**4** are obviously less negative than those of the corresponding free ligands, indicating that the boron chelation can greatly lower the

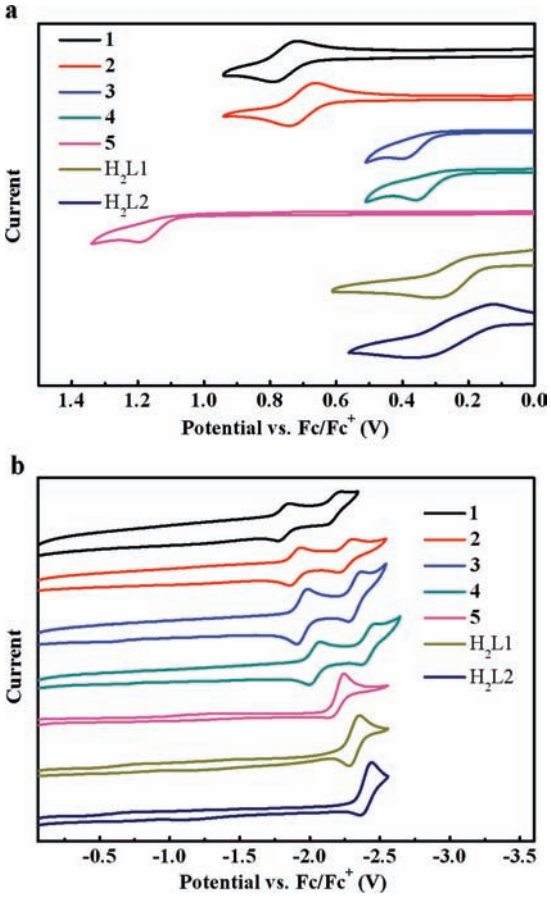

Figure 5. Cyclic voltammograms of **1**−**5**, H_2L1, and H_2L2: (a) anodic runs; (b) cathodic runs.

Table 2. Electrochemical Data [a] and HOMO/LUMO Energy Levels

			experimental data		DFT calculations	
compd	$E_{ox}^{1/2}$ (V)[b]	$E_{red}^{1/2}$ (V)[c]	HOMO (eV)	LUMO (eV)	HOMO (eV)	LUMO (eV)
1	+0.75	−1.81	−5.55	−2.99	−5.35	−2.46
2	+0.70	−1.89	−5.50	−2.91	−5.25	−2.34
3	+0.40[d]	−1.94	−5.06[e]	−2.86	−4.99	−2.31
4	+0.36[d]	−2.03	−5.01[e]	−2.77	−4.88	−2.19
5	+1.20[d]	−2.24[d]			−5.80	−1.96
H_2L1	+0.30[d]	−2.32	−5.21[e]	−2.48		
H_2L2	+0.37[d]	−2.40	−5.17[e]	−2.40		

[a] Potentials are given against ferrocene/ferrocenium (Fc/Fc^+). [b] Measured in CH_2Cl_2. [c] Measured in DMF. [d] Peak potential. [e] From the optical bandgap and the LUMO energy.

lowest unoccupied molecular orbital (LUMO) level of the π-system. Notably, the first reduction potentials of compounds **1**−**4** are less negative than that of Alq_3 (E_{pc} = −2.3 V),[22] one of the most widely used electron-transporting materials, which might be indicative of the good electron-transporting properties of these compounds in EL devices. By replacing the phenyl groups in compounds **1** and **2** with ethyl groups, in compounds **3** and **4**, the reduction potentials show a slight negative shift.

All these diboron compounds **1**−**4** have a large negatively shifted oxidation wave compared with the

(20) Cui, Y.; Wang, S. *J. Org. Chem.* **2006**, *71*, 6485.
(21) (a) Wu, J.; Abu-Omar, M. M.; Tolbert, S. H. *Nano Lett.* **2001**, *1*, 27. (b) Nicola, A. D.; Liu, Y.; Schanze, K. S.; Ziessel, R. *Chem. Commun.* **2003**, 288. (c) Lees, A. J. *Coord. Chem. Rev.* **1998**, *177*, 3.

(22) Shinar, J. *Organic light-emitting devices: a survey*; Springer-Verlag New York, Inc.: New York, 2003.

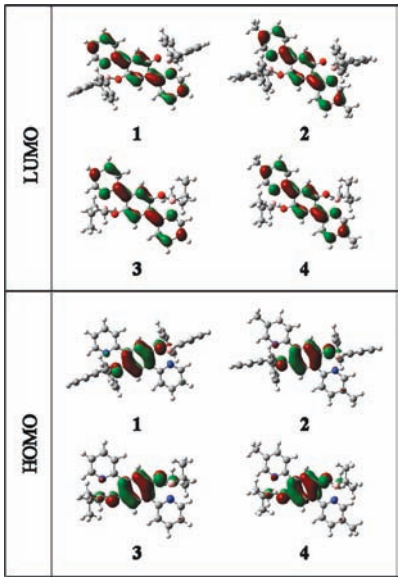

Figure 6. Calculated frontier orbitals for **1**−**4**.

monoboron compound, for instance, **3** and **4** exhibit an irreversible oxidation wave with peak potentials at +0.40 and +0.36 V, respectively, which are negatively shifted by about 0.80 V as compared with that of **5** (E_{pa} = +1.20 V). This result shows the significant effect of the diboron-contained ladder π-conjugated skeleton. The oxidation potentials of these ladder-type boron compounds are in general more positive than those of the corresponding free ligands. Compounds **3** and **4** with ethyl groups on boron atoms have a decreased oxidation potential compared with **1** and **2**, respectively, which might be due to the electron-donating properties of the ethyl groups. Worth noting is that **1** and **2** show reversible oxidation waves. This is in contrast to the cases of **3** and **4**, which only show irreversible oxidation waves. The stability of the oxidized species of these diboron compounds is dependent on the substituents on boron centers, namely, the phenyl groups stabilize the produced radical cation while the ethyl groups do not.

Molecular Orbital Calculations. To further understand the electronic structures of compounds **1**−**4**, we carried out density functional theory (DFT) calculations for these compounds, together with that of compound **5** for comparison. All diboron compounds **1**−**4** have a higher highest occupied molecular orbital (HOMO) level and a lower LUMO level compared with the monoboron compound **5** (Table 2), which is consistent with the electrochemical data. Figure 6 shows the HOMO and LUMO plots of compounds **1**−**4**. The HOMOs are mainly donated by the π-orbitals of quinol moiety, while the LUMOs are predominated by the π*-orbitals of the whole ligand (L1 or L2). The orbital components of HOMO and LUMO are shown in Supporting Information, Table S3. Compounds **3** and **4** with ethyl groups on the boron atom show a significantly higher HOMO level and a slightly higher LUMO level compared with the phenyl-substituted compounds **1** and **2**, respectively. This result also agrees well with the electrochemical data. The increased HOMO and LUMO levels of the ethyl-substituted compounds

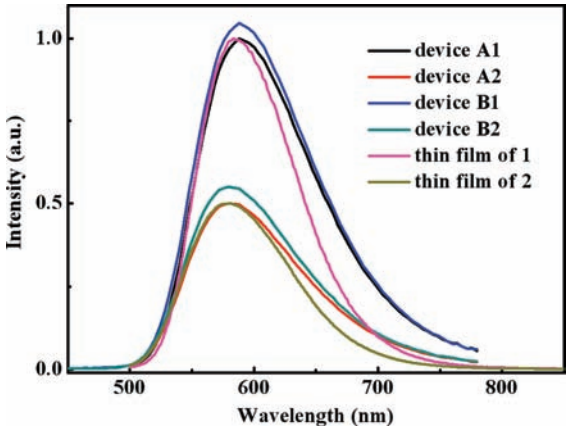

Figure 7. EL spectra of the devices and PL spectra of thin films of **1** and **2**.

Table 3. Data of Electroluminescent Devices

device	λ_{max} (nm)	turn-on voltage (V)	maximum luminance (Cd/m^2)	maximum efficiency (Cd/A)
A1	588	2.6	8156	2.03
A2	580	3.2	8505	2.56
A5	485	14.0	9	0.07
B1	588	2.4	8438	2.18
B2	580	2.5	9754	4.04
B5	484	10.0	264	0.69

should be attributed to the electron-donating properties of the ethyl group, which will lead to an increased electron density at the ligand skeleton. A similar effect of substituents attached to boron on the HOMO and LUMO levels was observed in a class of borondipyrromethene dyes.[23]

Electroluminescent Properties. Considering the high thermal stabilities, intensive emissions, and strong electron-accepting properties of compounds **1** and **2**, we thus fabricated two types of devices to evaluate their EL characteristics. The first one was a double-layer device with the configuration of [ITO/NPB (40 nm)/**1** or **2** (70 nm)/LiF (0.5 nm)/Al (200 nm)] (devices A1 and A2) in which NPB was used as the hole-transporting material, and compound **1** or **2** acted as both the emitter and the electron-transporting material. These devices produced orange electroluminescence with peaks centered at 588 and 580 nm for A1 and A2, respectively. The EL spectra of both devices matched well with the thin-film PL spectra of corresponding boron compounds, indicating that the EL luminescence originated from the intrinsic emissions of these compounds, as shown in Figure 7. It is worth noting that only a few non-doped orange or red emission OLEDs fabricated by using boron-contained emitting materials have been reported previously.[7d,8b,8d] The turn-on voltages were quite low and reached 2.6 and 3.2 V for devices A1 and A2, respectively. Device A1 could reach a maximum brightness of 8156 cd/m^2 at 11 V, and a maximum current efficiency of 2.03 cd/A at 6.5 V. The brightness and current efficiency of A2, summarized in Table 3, are comparable to those of A1. The EL performance of

(23) Goze, C.; Ulrich, G.; Mallon, L. J.; Allen, B. D.; Harriman, A.; Ziessel, R. *J. Am. Chem. Soc.* **2006**, *128*, 10231.

compounds **1** and **2** are at high level in comparison with those of the previously reported four-coordinate boron compounds.[7−9] The second type of devices we fabricated was the typical three-layer device with the configuration of [ITO/NPB (40 nm)/**1** or **2** (60 nm)/Alq_3 (10 nm)/LiF (0.5 nm)/Al (200 nm)] (devices B1 and B2), in which an additional Alq_3 material was used as the electron-transport layer. The EL spectra of devices B1 and B2 were nearly the same as those of the double layer devices A1 and A2 (Figure 7), respectively, indicating that the EL emissions of the three-layer devices also originated from the boron compounds. The EL performance of B1 and B2 are summarized in Table 3. Device B1 exhibited similar performance to the double-layer device A1, while device B2 showed higher brightness and efficiency than device A2. In fact, device B2 with the maximum brightness of 9754 cd/m^2 is one of the brightest EL devices fabricated by using boron-contained emitting materials. Worth noting is that although compound **5** has higher PL efficiency compared with **1** and **2**, the double-layer (A5) and three-layer (B5) devices based on **5** with the same configurations as devices A1 and B1, respectively, have much lower EL brightness and efficiencies (Table 3). Devices A5 and B5 display blue-green color emission at around 485 nm. This comparison demonstrates the superiority of boron compounds with ladder structure as EL materials.

Conclusion

We have designed and synthesized four boron-contained ladder-type compounds **1**−**4**. Incorporating two boron atoms into the ladder-type π-conjugated skeletons endows these materials with high thermal stability and strong electron affinity. For compounds **1** and **2**, the PL quantum yield in the solid-state does not show significant decrease as compared with that in solution, which is attributed to the steric hindrance of the bulky BPh_2 groups. Simple double-layer EL devices fabricated using materials **1** and **2** as both emitters and electron-transporting layers displayed good performance. We suggest that the ladder-type boron compounds are a class of promising candidates for applications in OLEDs. Further modification on this boron-contained ladder-type π-conjugated system is ongoing in our laboratory.

Acknowledgment. This work was supported by the National Natural Science Foundation of China (50733002), the Major State Basic Research Development Program (2009CB623600), the 863 Project (2006AA03A162) and 111 Project (B06009).

Supporting Information Available: ^1H NMR spectra of compounds **1**−**5**, ORTEP drawing of **1**, $J-V$ and $L-V$ characteristics of the EL devices, crystallographic data for **1** and **3** in PDF and CIF formats, and the orbital components of HOMO and LUMO for compounds **1**−**4**. This material is available free of charge via the Internet at http://pubs.acs.org.